THE JOURNAL OF BIOLOGICAL CHEMISTRY VOL. 291, NO. 48, pp. 24838–24850, November 25, 2016
Published in the U.S.A.

RANKL (Receptor Activator of NFκB Ligand) Produced by Osteocytes Is Required for the Increase in B Cells and Bone Loss Caused by Estrogen Deficiency in Mice*[S]

Received for publication, June 7, 2016, and in revised form, September 25, 2016 Published, JBC Papers in Press, October 12, 2016, DOI 10.1074/jbc.M116.742452

Yuko Fujiwara[‡§], Marilina Piemontese[‡§], Yu Liu[‡§], Jeff D. Thostenson[¶], Jinhu Xiong[‡§], and Charles A. O'Brien[‡§1]

From the [‡]Center for Osteoporosis and Metabolic Bone Diseases and [¶]Department of Biostatistics, University of Arkansas for Medical Sciences and [§]Central Arkansas Veterans Healthcare System, Little Rock, Arkansas 72205

Edited by Luke O'Neill

The cytokine receptor activator of NFκB ligand (RANKL) produced by osteocytes is essential for osteoclast formation in cancellous bone under physiological conditions, and RANKL production by B lymphocytes is required for the bone loss caused by estrogen deficiency. Here, we examined whether RANKL produced by osteocytes is also required for the bone loss caused by estrogen deficiency. Mice lacking RANKL in osteocytes were protected from the increase in osteoclast number and the bone loss caused by ovariectomy. Moreover, these mice did not exhibit the increase in bone marrow B lymphocytes caused by ovariectomy that occurred in control littermates. Deletion of estrogen receptor α from B cells did not alter B cell number or bone mass and did not alter the response to ovariectomy. In addition, lineage-tracing studies demonstrated that B cells do not act as osteoclast progenitors in estrogen-replete or estrogen-deficient mice. Taken together, these results demonstrate that RANKL expressed by osteocytes is required for the bone loss as well as the increase in B cell number caused by estrogen deficiency. Moreover, they suggest that estrogen control of B cell number is indirect via osteocytes and that the increase in bone marrow B cells may be a necessary component of the cascade of events that lead to cancellous bone loss during estrogen deficiency. However, the role of B cells is not to act as osteoclast progenitors but may be to act as osteoclast support cells.

Osteoclasts are bone resorbing cells derived from myeloid progenitors in the bone marrow (1). The cytokine receptor activator of NFκB ligand (RANKL),[2] encoded by the *Tnfsf11* gene, is essential for osteoclast formation but plays important roles in other processes such as mammary gland and lymphocyte development (2, 3). Consistent with this, RANKL is produced by a variety of different cell types and in response to many different stimuli (4). Osteocytes are cells that live in mineralized bone and are derived from osteoblasts, which produce bone matrix (5). Gene deletion studies in mice have demonstrated that osteocytes are an essential source of the RANKL involved in osteoclast formation under physiological conditions as well as in response to biomechanical unloading and dietary calcium deficiency (6–8).

Estrogen deficiency in mice increases osteoclast number on cancellous and cortical bone and causes bone loss in both compartments (9). Estrogen deficiency also causes a striking increase in B lymphocyte number in the bone marrow (10, 11). Moreover, deletion of the *Tnfsf11* gene from B cells prevents both the increase in B cell number and the increase in cancellous osteoclast number caused by ovariectomy (12). These findings suggest that estrogen may suppress osteoclast number in part by suppressing B cell number in the bone marrow.

How B cells might contribute to osteoclast formation during estrogen deficiency is unclear. On the one hand, RANKL produced by B cells may directly interact with its receptor RANK on osteoclast progenitors and thereby stimulate osteoclast formation. On the other hand, several independent studies have demonstrated that purified populations of B cells can be induced to differentiate into osteoclasts when exposed to recombinant RANKL *in vitro* (13–17). Thus, B cells may act as a source of osteoclast progenitors, at least under some conditions. However, there has been no evidence that this phenomenon occurs *in vivo* either in estrogen-replete or estrogen-deficient conditions.

The goal of the current study was to determine whether RANKL produced by osteocytes contributes to the elevated osteoclast formation and bone loss caused by estrogen deficiency. We found that this is the case but that deletion of the *Tnfsf11* gene from osteocytes also prevented the increase in B cell production caused by estrogen deficiency, suggesting that estrogen controls B cell number indirectly. Consistent with this, we found that deletion of estrogen receptor α (ERα), encoded by the *Esr1* gene, from B cells had no effect on B cell number. Lastly, we used *in vivo* lineage-tracing studies to investigate the possibility that cells committed to the B cell lineage

* This work was supported, in whole or in part, by National Institutes of Health Grants P01 AG13918 and R01 AR49794 and the University of Arkansas for Medical Sciences Translational Research Institute (NIH UL1TR000039). This work was also supported by the Department of Veterans Affairs Biomedical Laboratory Research and Development Service Grant I01 BX000294 and by tobacco settlement funds. C. A. O'Brien owns stock in Radius Health Inc. The content is solely the responsibility of the authors and does not necessarily represent the official views of the National Institutes of Health.

[S] This article contains supplemental Figs. S1–S3.

[1] To whom correspondence should be addressed: University of Arkansas for Medical Science, 4301 W. Markham St., Little Rock, AR 72205. Tel.: 501-686-5607; Fax: 501-686-8148; E-mail: caobrien@uams.edu.

[2] The abbreviations used are: RANKL, receptor activator of NFκB ligand; ERα, estrogen receptor α; BMM, bone marrow macrophage; CAR, Cxcl12-abundant reticular; μCT, microcomputed tomography; FAM, 6-carboxyfluorescein; TRAP, tartrate-resistant acid phosphatase.

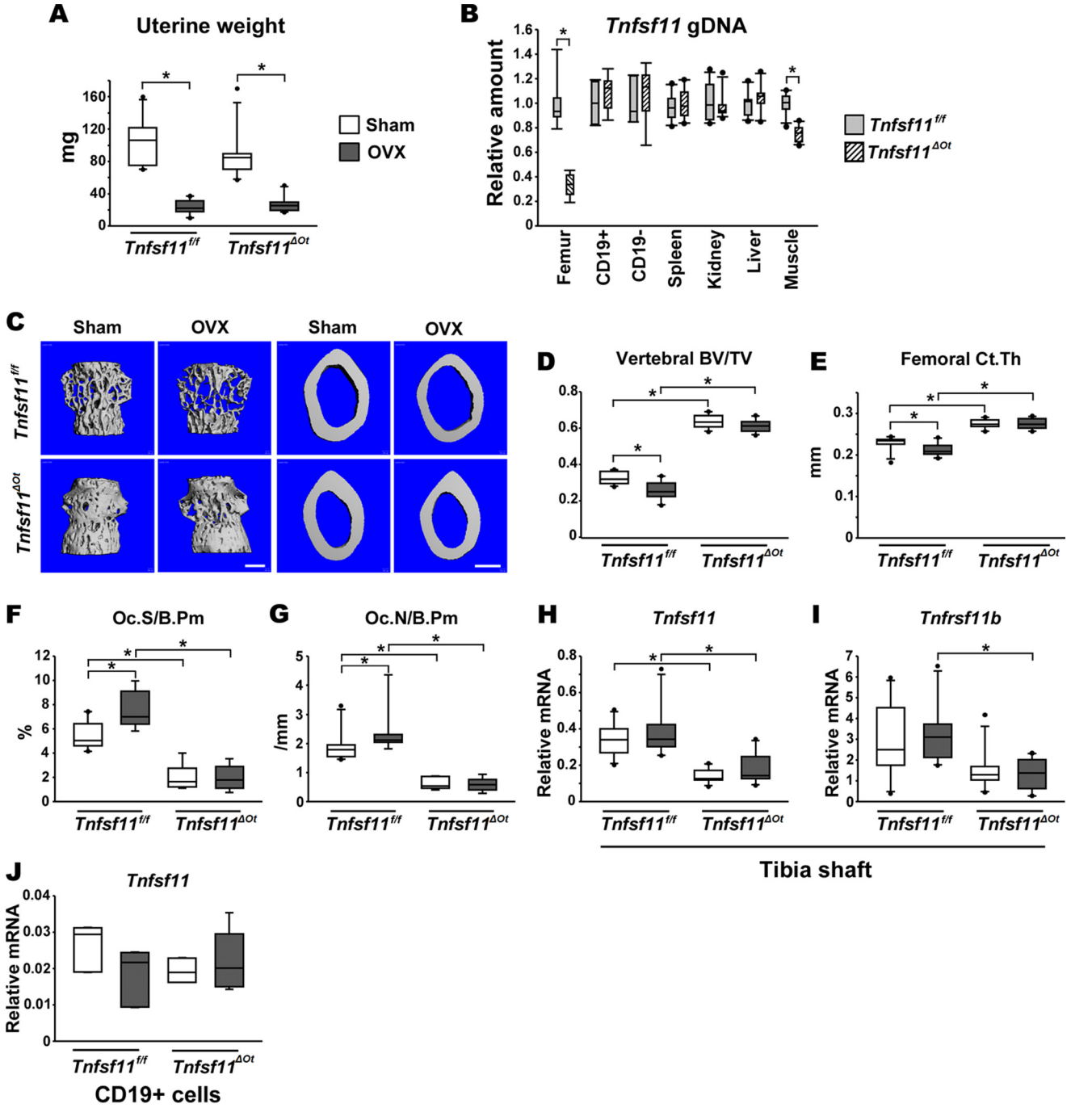

FIGURE 1. **Deletion of *Tnfsf11* from osteocytes prevents ovariectomy-induced bone loss.** 6-Month-old female Tnfsf11$^{f/f}$ and Tnfsf11$^{\Delta Ot}$ mice were either sham-operated (*white bars*) or ovariectomized (*OVX*) (*dark gray bars*) and killed 6 weeks later. *A*, uterine weight ($n = 10–12$ animals per group). *B*, real time PCR quantification of *Tnfsf11* genomic DNA in femoral cortical bone, CD19+ bone marrow cells, CD19− bone marrow cells, spleen, kidney, liver, and muscle ($n = 3–12$). *C*, μCT images of vertebral cancellous bone and femoral cortical bone. *Bar* = 500 μm. *D*, bone volume over tissue volume (*BV/TV*) of cancellous bone measured in lumbar vertebra by μCT ($n = 10–12$). *E*, cortical thickness of the femoral midshaft measured by μCT ($n = 10–12$). *F* and *G*, osteoclast surface per bone perimeter (*Oc.S/B.Pm*) and osteoclast number per bone perimeter (*Oc.N/B.Pm*) measured by histomorphometric analysis of lumbar vertebra ($n = 6–10$). *H* and *I*, real time RT-PCR of *Tnfsf11* and *Tnfrsf11b* mRNA in tibial cortical bone ($n = 10–12$). *J*, *Tnfsf11* mRNA expression in CD19+ bone marrow cells ($n = 3–5$). *, $p < 0.05$.

can act as osteoclast progenitors and found that this was not the case.

Results

Osteocyte RANKL Is Required for Ovariectomy-induced Bone Loss—To determine whether RANKL production by osteocytes is required for the bone loss caused by estrogen deficiency, adult female mice lacking the *Tnfsf11* gene in osteocytes (hereafter referred to as Tnfsf11$^{\Delta Ot}$) and their control littermates (hereafter referred to as Tnfsf11$^{f/f}$) underwent either a sham operation or ovariectomy. Six weeks after the operations, ovariectomized mice had lower uterine weight than sham-operated mice, confirming estrogen deficiency (Fig. 1*A*). Quantification of the *Tnfsf11* locus in genomic DNA from tissues harvested

from the sham-operated mice confirmed deletion of the gene in osteocyte-enriched bones but also revealed a small but significant deletion in muscle tissue (Fig. 1*B*). However, RANKL mRNA levels were >100-fold lower in muscle compared with bone tissue and were not altered by ovariectomy, arguing against any functional contribution of muscle-derived RANKL to bone resorption (supplemental Fig. 1).

Ovariectomy led to reduced vertebral cancellous bone volume and femoral cortical thickness in Tnfsf11$^{f/f}$ mice but not Tnfsf11$^{\Delta Ot}$ mice (Fig. 1, *C–E*). However, as noted in previous studies, both of these parameters were elevated in sham-operated Tnfsf11$^{\Delta Ot}$ mice compared with sham-operated Tnfsf11$^{f/f}$ littermates. Histological analysis of vertebral cancellous bone revealed that ovariectomy increased osteoclast number and surface in Tnfsf11$^{f/f}$ mice, but this did not occur in Tnfsf11$^{\Delta Ot}$ mice, which had fewer osteoclasts than Tnfsf11$^{f/f}$ mice, when compared with the sham-operated groups (Fig. 1, *F–G*). As expected from *Tnfsf11* gene deletion, RANKL mRNA levels were lower in cortical bone from Tnfsf11$^{\Delta Ot}$ mice but were not changed by ovariectomy in either these mice or control littermates (Fig. 1*H*). Osteoprotegerin mRNA levels were also lower in Tnfsf11$^{\Delta Ot}$ mice but were unchanged by ovariectomy (Fig. 1*I*). In addition and consistent with our earlier report, ovariectomy did not change RANKL mRNA in B lymphocytes in Tnfsf11$^{f/f}$ or Tnfsf11$^{\Delta Ot}$ mice (Fig. 1*J*). These results demonstrate that RANKL produced by osteocytes is essential for the increase in osteoclast number and the bone loss caused by estrogen deficiency but that this occurs without significant changes in RANKL or osteoprotegerin production.

Osteocyte RANKL Is Required for the Increase in B Cells after Ovariectomy—We have shown previously that deletion of RANKL from B lymphocytes prevents the increase in bone marrow B cells and cancellous osteoclasts after ovariectomy (12). This observation suggested a possible link between the two phenomena. To determine if this relationship was present in mice lacking RANKL in osteocytes, we used flow cytometry to measure bone marrow B lymphocytes in the sham-operated and ovariectomized Tnfsf11$^{\Delta Ot}$ and Tnfsf11$^{f/f}$ mice. Although the expected increase in B cells occurred in Tnfsf11$^{f/f}$ mice, it did not occur in Tnfsf11$^{\Delta Ot}$ mice (Fig. 2*A*). T lymphocyte and erythrocyte progenitor percentages were not altered by ovariectomy in either genotype, but the percentage of monocytes was slightly reduced only in Tnfsf11$^{f/f}$ mice (Fig. 2, *B–D*). The effect on monocytes has been observed previously and is likely a consequence of the increase in the percentage of B cells (11). Supporting this idea, the total number of B cells isolated by magnetic bead separation was elevated in ovariectomized Tnfsf11$^{f/f}$ but not Tnfsf11$^{\Delta Ot}$ mice (Fig. 2*E*). These results also demonstrated a trend toward reduced B lymphocyte number under estrogen-replete conditions, but the differences were not significant possibly due to the small effect size and limited number of samples. Therefore, we measured the percentage of bone marrow B cells in a larger number of intact (no operation) Tnfsf11$^{f/f}$ and Tnfsf11$^{\Delta Ot}$ mice and found that the percentage of these cells was indeed lower in Tnfsf11$^{\Delta Ot}$ mice (Fig. 2*F*).

Osteocyte RANKL may promote B cell number in the bone marrow by binding to RANK on B cells to promote their proliferation or survival. However, deletion of RANK from B cells does not alter B cell number indicating that RANK signaling in another cell type mediates the effects of RANKL on B cells (19). Our observation that *Tnfsf11* mRNA in osteocyte-enriched bone was not altered by ovariectomy also argues against such a scenario. Alternatively, osteocyte RANKL could indirectly control B cell number by controlling the number of osteoblast-lineage cells. Osteoblasts increase after ovariectomy in response to increased bone resorption, a phenomenon known as coupling (20). Moreover, osteoblasts provide factors such as IL-7 and CXCL-12 that support B cell development (21–24). Consistent with the idea that the failure to increase B cells was due to reduced support by osteoblast-lineage cells, *IL-7* mRNA in bone was increased by ovariectomy in Tnfsf11$^{f/f}$ but not Tnfsf11$^{\Delta Ot}$ mice (Fig. 2*G*). A similar trend was observed for *CXCL-12* mRNA (Fig. 2*H*).

Estrogen Indirectly Suppresses B Cell Number—The requirement of osteocyte RANKL for the increase in B cells by estrogen deficiency suggests that estrogen controls B cell number indirectly. However, it is possible that a direct effect is also required. To address this question, we deleted ERα, encoded by the *Esr1* gene, from B lymphocytes using CD19-Cre mice, which delete target genes early in the B cell lineage (25). Deletion of the conditional *Esr1* allele occurred specifically in bone marrow CD19+ cells (Fig. 3*A*). Moreover, estrogen receptor β mRNA, encoded by *Esr2*, was undetectable in this cell population and not up-regulated by *Esr1* deletion (Fig. 3*B*).

We then compared the effect of *Esr1* deletion on the skeleton and bone marrow B cells in sham-operated and ovariectomized adult mice. Reduced uterine weight confirmed estrogen deficiency in the ovariectomized groups of both Esr1$^{f/f}$ and Esr1$^{\Delta B}$ mice (Fig. 3*C*). Deletion of *Esr1* from B cells did not alter bone mass or the loss of bone caused by ovariectomy (Fig. 3, *D–F*). Importantly, the percentage of CD19+ B cells in the bone marrow was not affected by *Esr1* deletion, nor was the increase in B cells caused by ovariectomy (Fig. 3*G*). Moreover, quantification of several stages of B lymphocyte development also showed no difference between genotypes (Fig. 3, *H–K*). Taken together, these results argue against a direct effect of estrogen on B cell number in the bone marrow in either estrogen-replete or estrogen-deficient mice.

B Cells Do Not Act as Osteoclast Progenitors—Our findings that *Tnfsf11* deletion from either B cells or osteocytes prevents the increase in both B cells and osteoclasts caused by ovariectomy supports the idea that the increase in these two cell types may be functionally linked. Many previous studies have shown that isolated B cells can act as osteoclast progenitors when cultured *in vitro* with M-CSF and RANKL. However, the ability of B cells to act as osteoclast progenitors *in vivo* has not been demonstrated. Therefore, we used lineage-tracing studies to determine whether cells committed to the B lymphocyte lineage could be redirected to the myeloid-osteoclast lineage either in the estrogen-replete or estrogen-deficient state.

First we confirmed that preparations of CD19+ B cells isolated from mouse bone marrow by magnetic beads could be induced to form osteoclasts *in vitro* after exposure to M-CSF and RANKL (Fig. 4*A*). We found that CD19+ cells isolated to 96% purity formed osteoclasts under these conditions but that

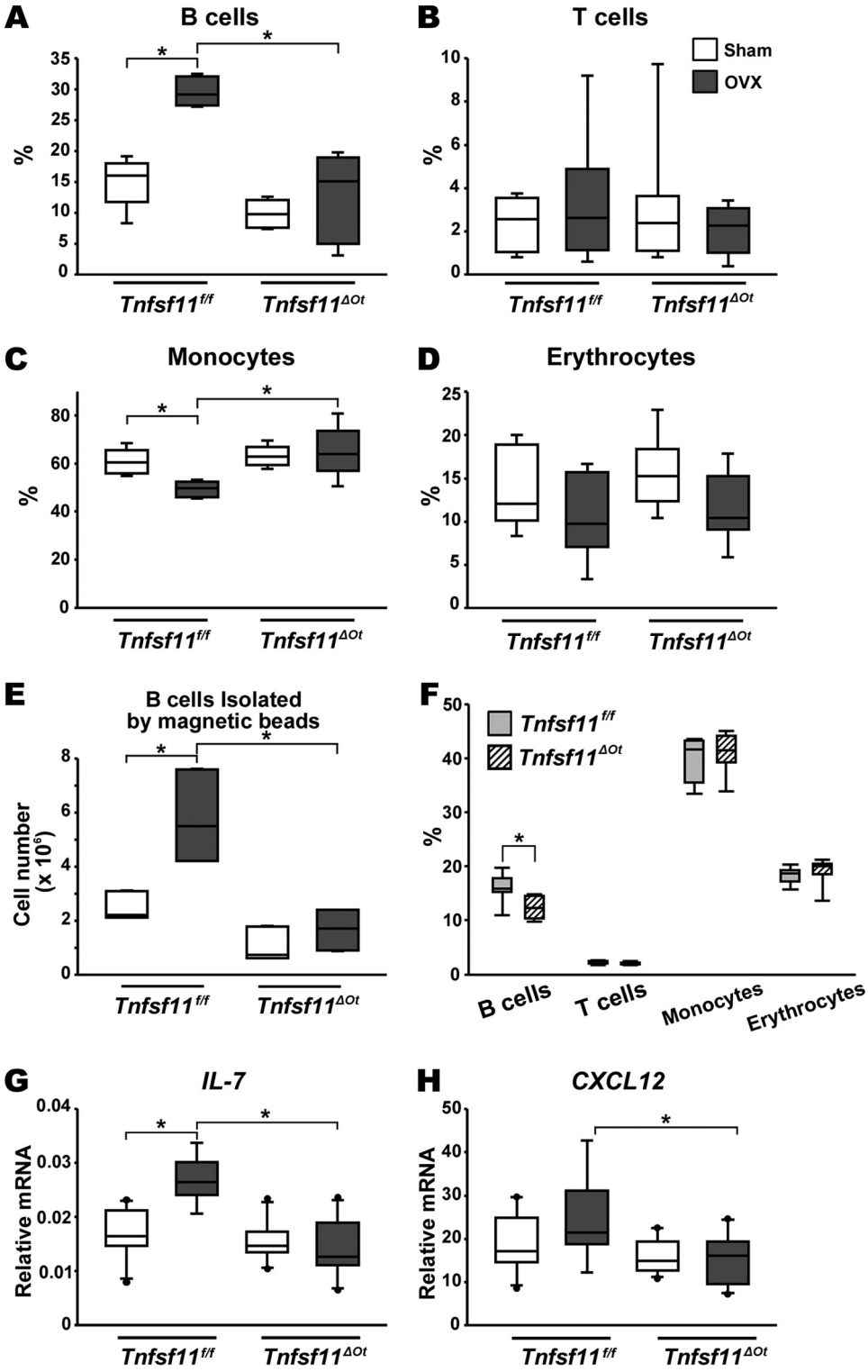

FIGURE 2. **Deletion of *Tnfsf11* from osteocytes prevents the increase in bone marrow B cells after ovariectomy.** *A–D*, percentage of B cells, T cells, monocytes, and erythrocyte progenitors in bone marrow analyzed by flow cytometry ($n = 5–6$). *OVX*, ovariectomized. *E*, bone marrow cells isolated using anti-CD19 magnetic beads were counted using a cellometer Auto 2000 (Nexcelom Bioscience) ($n = 3$). *F*, percentage of B cells, T cells, monocytes, and erythrocytes in bone marrow of Tnfsf11$^{f/f}$ and Tnfsf11$^{\Delta Ot}$ mice by flow cytometry ($n = 8$). *G* and *H*, real time RT-PCR of *IL-7* and *CXCL12* mRNA in lumbar vertebra ($n = 9–11$). *, $p < 0.05$.

this required a higher concentration of cells and longer incubation time than CD19− cell preparations (Fig. 4, *A–C*). The requirement for different conditions could be due to the need for B cells to undergo a lineage switch. Alternatively, the osteoclasts in these cultures may form from contaminating myeloid-lineage cells, and the higher cell number and culture period may be required for these cells to expand to sufficient numbers for osteoclast formation.

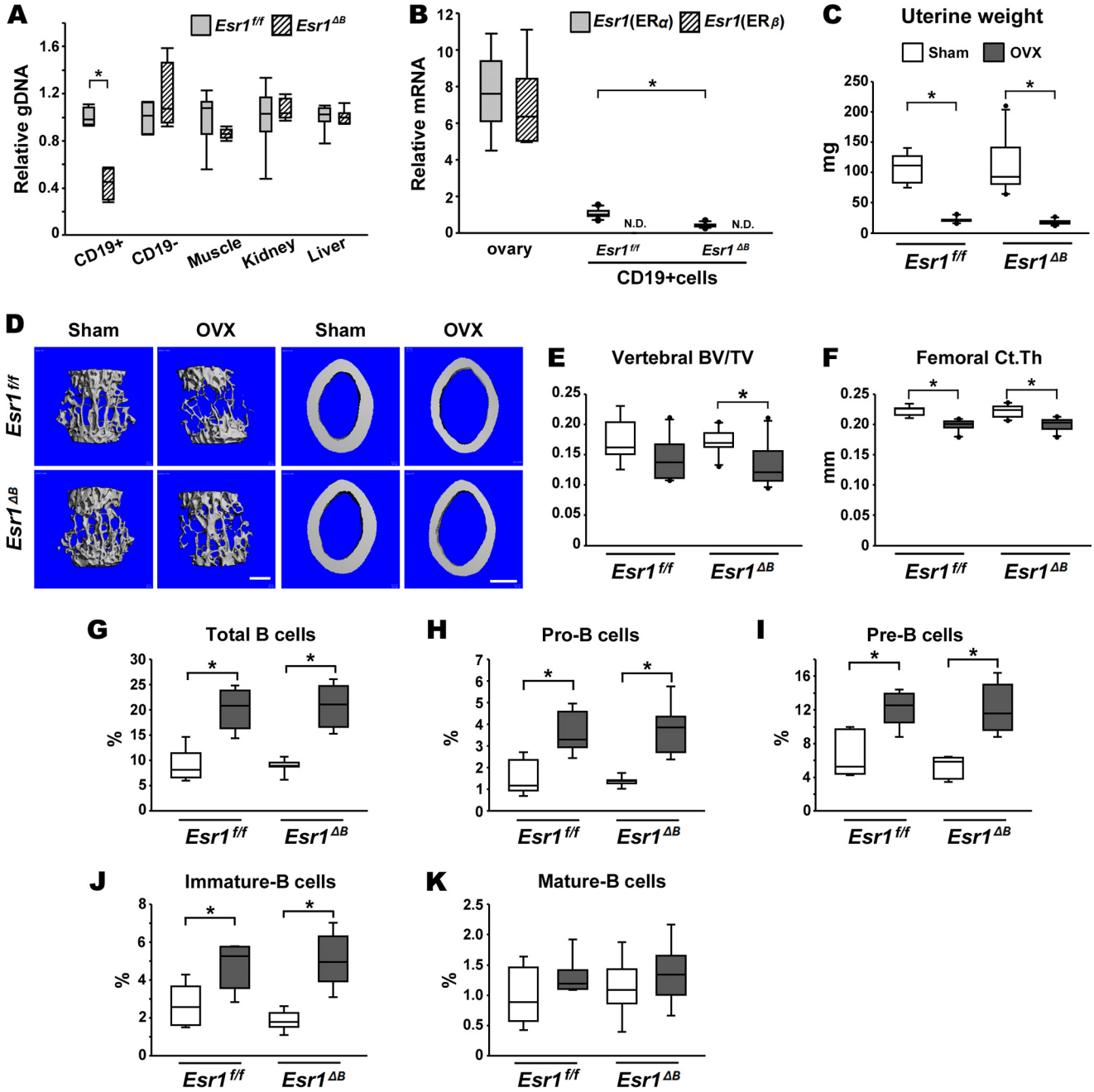

FIGURE 3. **Deletion of *Esr1* from B cells does not alter bone mass or B cell number.** 6-Month-old female $Esr1^{f/f}$ and $Esr1^{\Delta B}$ mice were either sham-operated or ovariectomized (*OVX*) and killed 6 weeks later. *A*, real time PCR quantification of *Esr1* genomic DNA in CD19+ cells, CD19− cells, muscle, kidney, and liver (n = 3–8). *B*, real time RT-PCR of *Esr1* and *Esr2* mRNA in ovary and CD19+ cells in $Esr1^{f/f}$ and $Esr1^{\Delta B}$ mice (n = 6–11). *N.D.*, not detected. *C*, uterine weight (n = 9–13 animals per group). *D*, μCT images of vertebral cancellous bone and femoral cortical bone. *Bar* = 500 μm. *E*, bone volume over tissue volume (*BV/TV*) of cancellous bone measured in lumbar vertebra by μCT (n = 9–13). *F*, cortical thickness of the femoral midshaft measured by μCT (n = 9–13). *G–K*, percentage of B cell populations in bone marrow measured by flow cytometry: total B cells ($B220^{+}/CD19^{+}$), pro-B cells ($B220^{lo}/CD43^{+}/CD19^{+}/IgM^{-}$), pre-B cells ($B220^{lo}/CD43^{-}/CD19^{+}/IgM^{-}$), immature B cells ($B220^{lo}/CD43^{-}/CD19^{+}/IgM^{+}$), mature B cells ($B220^{hi}/CD43^{-}/CD19^{+}/IgM^{+}$) ($n$ = 5–8). *, $p < 0.05$.

To determine if the osteoclasts in these cultures differentiated from cells of the B lymphocyte lineage, we crossed CD19-Cre mice, which cause recombination in all B cells, with tdTomato Cre-reporter mice. In the offspring of this cross, bone marrow B cells were efficiently and specifically labeled with the tdTomato fluorescent protein (supplemental Fig. 2). We performed ovariectomy or sham operations on these mice and isolated CD19-positive cells from bone marrow by magnetic beads (supplemental Fig. 2). Freshly isolated B cells from either sham-operated or ovariectomized mice displayed robust tdTomato fluorescence (Fig. 5*A*). However, the osteoclasts formed from these same preparations did not display tdTomato fluorescence (Fig. 5*B*), suggesting that the osteoclasts formed from contaminating myeloid-lineage cells. It is also possible that B cells and contaminating myeloid cells both contributed to osteoclast formation but that the fluorescence from the B cells was diluted to the point of being undetectable. To identify the lower limit of detection from such a contribution, we marked bone marrow

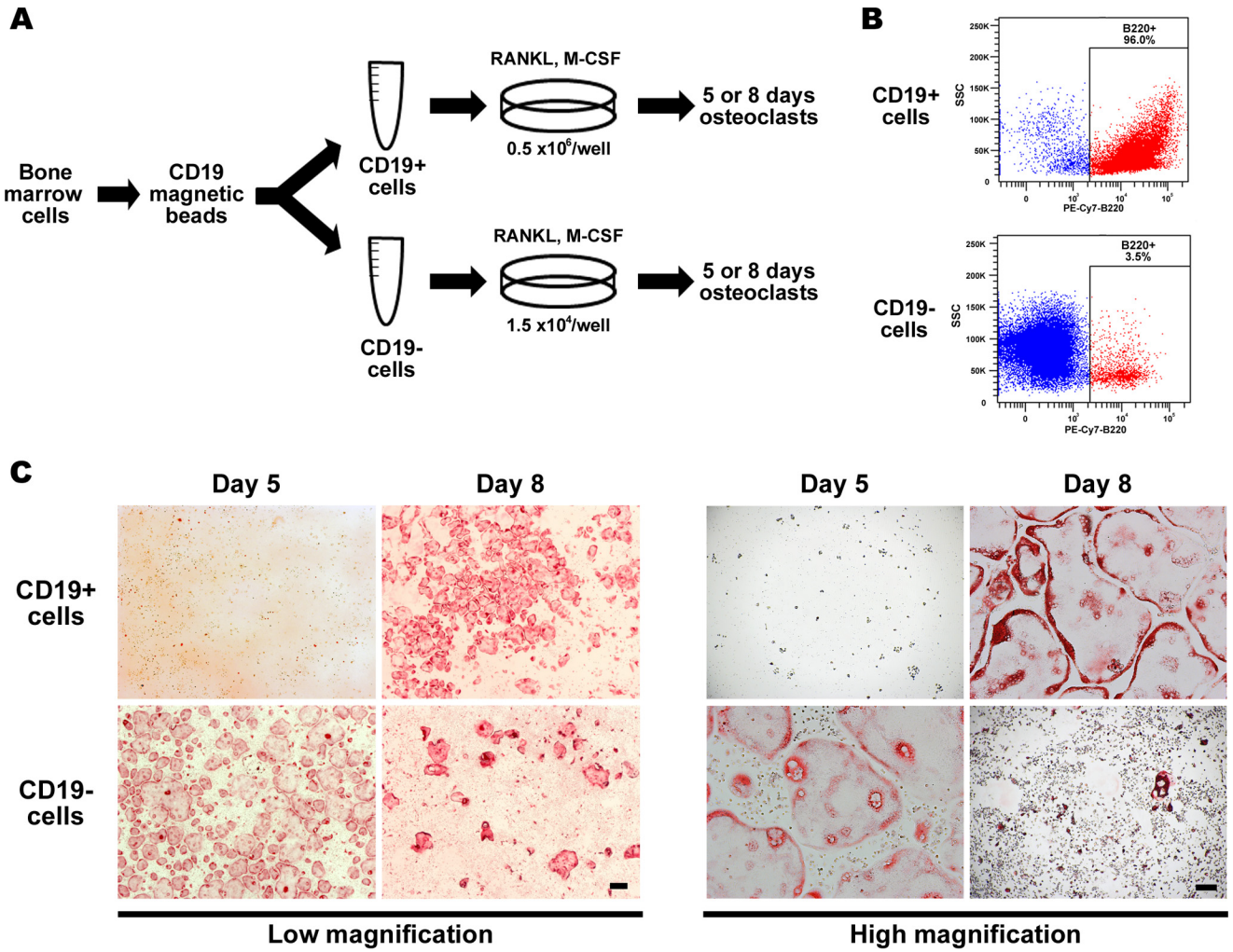

FIGURE 4. **Osteoclastogenic potential of B cell preparations.** *A*, diagram showing method to culture osteoclasts from isolated bone marrow cells. 5×10^5 CD19+ cells and 1.5×10^4 CD19− cells were plated per well of 48-well plates and cultured for 5 or 8 days. *B*, flow cytometric analysis of cells isolated by magnetic beads. *C*, TRAP staining of osteoclasts from CD19+ and CD19− cells after incubation with M-CSF and RANKL. *Left*, low magnification; *scale bar*, 200 μm. *Right*, high magnification; *scale bar*, 50 μm.

macrophages (BMMs) using LysM-Cre;tdTomato mice and mixed these with increasing amounts of unmarked BMMs and found that we could still detect tdTomato-positive osteoclasts even when only 2% of the cells in the culture were from LysMCre;tdTomato mice (Fig. 5*C*). Thus, the majority of osteoclasts formed in cultures from purified B cells are not derived from B cells but are likely derived from contaminating myeloid cells. More importantly, all osteoclasts on the cancellous bone surface of LysM-Cre;tdTomato mice were tdTomato-positive but none was positive in either sham-operated or ovariectomized CD19-Cre;tdTomato mice (Fig. 6 and supplemental Fig. 3). Based on these results we conclude that B cells do not differentiate into osteoclasts under normal physiological conditions or during estrogen deficiency.

Discussion

We have shown previously that RANKL produced by osteocytes is required for the increase in bone resorption caused by either hind limb unloading or dietary calcium deficiency (6, 8). Herein we show that osteocyte RANKL is also required for the increase in resorption caused by estrogen deficiency. One important difference between these earlier studies and the present work is that both unloading and calcium deficiency increase levels of *Tnfsf11* mRNA in osteocyte-enriched bone, but this did not occur with estrogen deficiency, nor were changes in *Tnfrsf11b* mRNA observed. Thus RANKL expression by osteocytes is permissive for the increase in osteoclast number and did not appear to be a direct target of estrogen. Consistent with this finding, deletion of ERα from osteocytes has no effect on osteoclast number (26, 27). We and others have shown that the amount of soluble RANKL protein in bone marrow supernatants does increase with either estrogen or androgen deficiency (12, 28, 29). However, whether this increase in soluble RANKL contributes to the increase in bone resorption caused by these conditions is unknown.

The *Dmp1-Cre* transgene used in this study also causes recombination in osteoblasts (6, 30). We have shown previously that deletion of *Tnfsf11* using a *Sost-Cre* transgene that does not delete in osteoblasts or lining cells leads to the same reduction in osteoclasts as deletion using the *Dmp1-Cre* transgene (30). Based on this, we concluded that osteocytes, not osteoblasts or lining cells, are the major source of RANKL involved in oste-

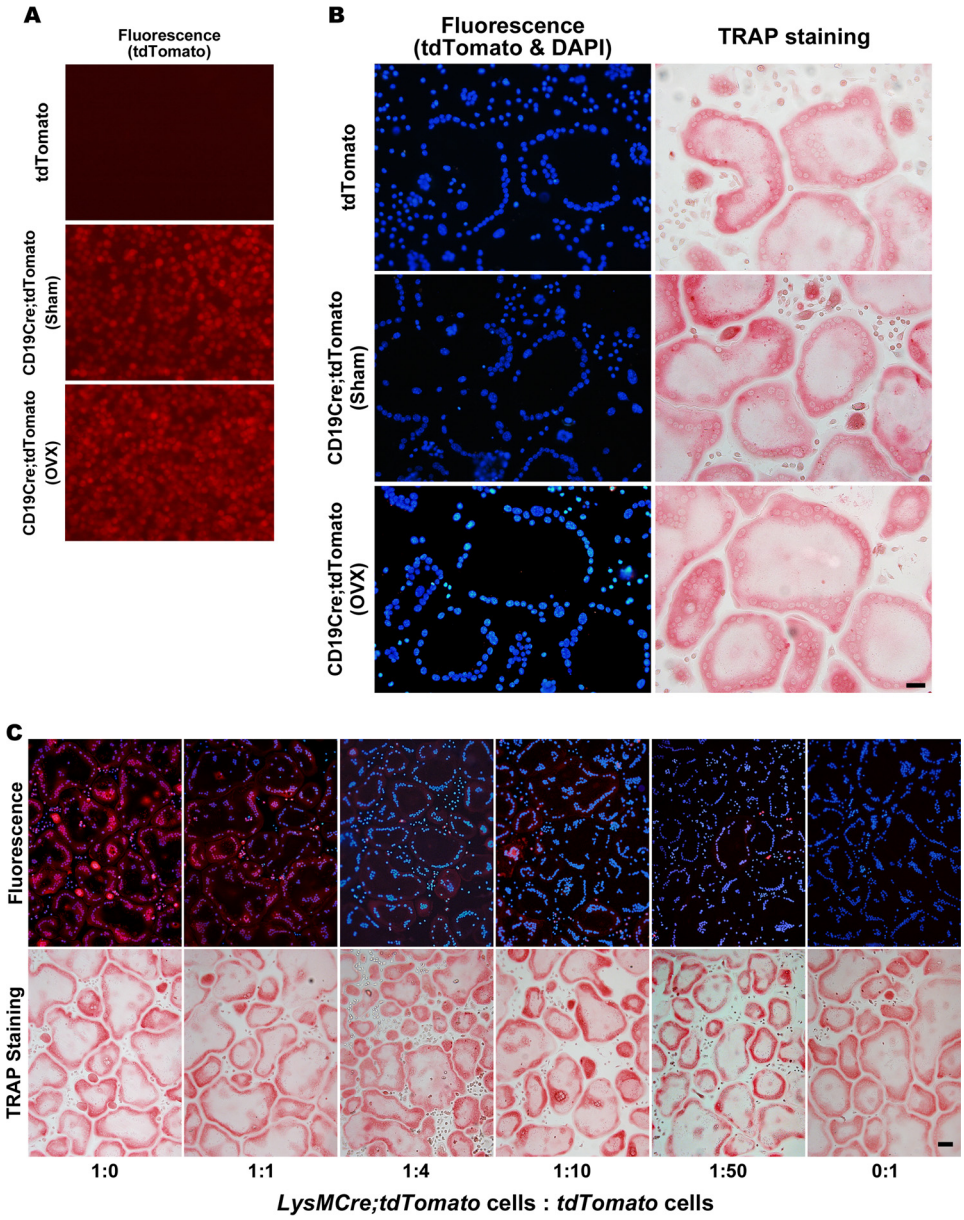

FIGURE 5. **CD19-Cre does not label osteoclasts *in vitro*.** *A*, images of tdTomato fluorescence in CD19+ cells immediately after isolation from mice of the genotypes indicated at the *left*. tdTomato fluorescence is in *red*, 20× magnification. *B*, fluorescent and brightfield images of osteoclasts in cultures of CD19+ cells from mice of the indicated genotypes after 8 days of culture. tdTomato fluorescence is in *red*, DAPI nuclear staining is in *blue*, and TRAP staining in the brightfield image is in *red*. *Scale bar*, 20 μm. *C*, fluorescence and brightfield images of osteoclast cultures containing different ratios of BMM from LysM-Cre;tdTomato and tdTomato mice. The ratio of LysM-Cre;tdTomato to tdTomato cells decreased from *left* to *right*. The *top panels* are fluorescent images with tdTomato fluorescence in *red* and DAPI fluorescence in *blue*. The *bottom panels* are brightfield images showing TRAP staining in *red*. *Scale bar*, 50 μm.

oclast formation. This finding together with our observation that *Tnfsf11* mRNA levels were unaffected by ovariectomy supports the conclusion that RANKL produced by osteocytes is responsible for supporting osteoclast formation in estrogen-replete and estrogen-deficient mice. It has been reported recently that the *Dmp1-Cre* transgene targets a subset of stromal cells designated Cxcl12-abundant reticular (CAR) cells (31). CAR cells are also targeted by an Osx1-Cre transgene (24), and we have shown that deletion of *Tnfsf11* using this same transgene beginning at 4 months of age does not alter osteoclast number (6), indicating that CAR cells do not supply RANKL for osteoclast formation.

We also found that osteocyte RANKL contributes to the number of B lymphocytes in the bone marrow of estrogen-replete mice and is required for the increase caused by estrogen deficiency. The latter finding was unexpected given that RANKL produced by B lymphocytes themselves is also required for this phenomenon (12). The mechanisms by which osteocyte RANKL controls B cell number are unclear but appear to be indirect as deletion of the receptor for RANKL from B cells does not alter B cell number (19). One possibility is that the low level of bone remodeling in $Tnfsf11^{\Delta Ot}$ mice may have reduced B cell number by reducing the amount of support factors supplied by osteoblast-lineage cells.

Consistent with this idea, multiple lines of evidence suggest that there is a linkage between the number of osteoblasts on cancellous bone and the number of B lymphocytes in the bone marrow. For example, ablation of osteoblasts reduces B cell

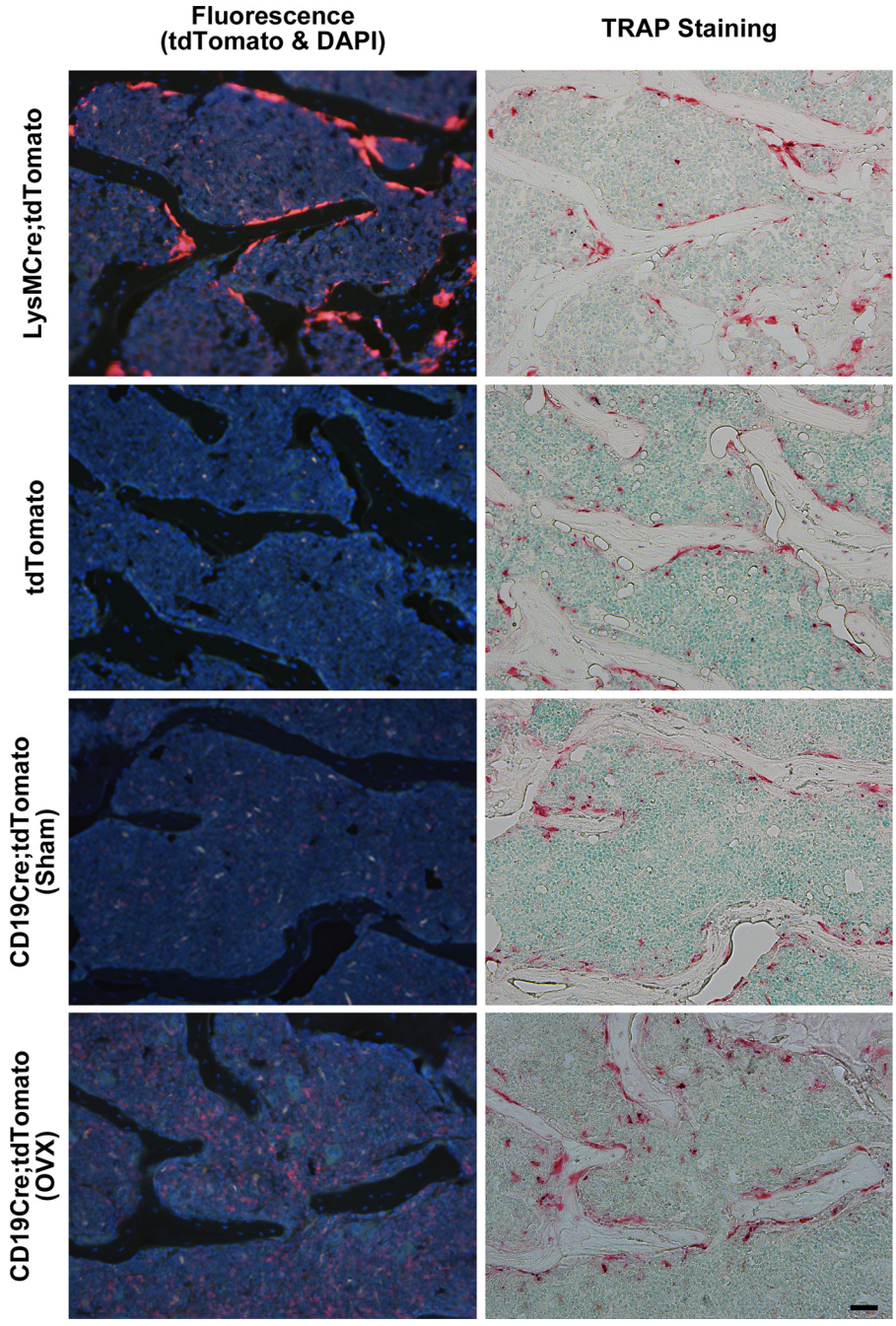

FIGURE 6. **CD19-Cre does not label osteoclasts *in vivo*.** Shown are fluorescence and bright field microscopy images of histological frozen sections of lumbar vertebra from LysM-Cre;tdTomato mice, tdTomato mice, and CD19-Cre;tdTomato mice. Images on the *left* are fluorescence showing tdTomato-positive cells in bone and bone marrow. Images on the *right* are brightfield images of the same sections after staining for TRAP activity. *Scale bar*, 20 μm.

number before reductions in other hematopoietic lineages (32). In addition, suppression of PTH receptor signaling specifically in osteoblasts reduces B cell number (22). Perhaps most relevant to the current work, suppression of bone remodeling by administration of bisphosphonates is sufficient to reduce the number of osteoblasts on the bone surface and the number of B cells in the bone marrow of mice (23, 33).

Many of these previous studies include evidence that osteoblast-lineage cells support B cell development by expressing *IL-7* and *CXCL-12* (22, 23, 32). We found that *IL-7* and *CXCL-12* mRNAs were elevated by ovariectomy in control mice but not in *Tnfsf11*$^{\Delta Ot}$ mice. Consistent with this, others have shown that IL-7 protein in bone marrow fluid is elevated at 7 or 14 days after ovariectomy (34, 35). These results together with evidence that osteoblast-lineage cells are an essential source of the IL-7 and CXCL-12 involved in B cell production (21, 24) support the idea that the failure to increase B cells in *Tnfsf11*$^{\Delta Ot}$ mice is a consequence of a failure to increase osteoblast number. It is also possible that cells of the osteoblast lineage are direct targets of estrogen, as *in vitro* studies have shown that estrogen suppresses B cell growth factors in bone marrow stromal cell cultures, which contain osteoblast progenitors (36, 37). It is also possible that the failure of these cytokines to increase in *Tnfsf11*$^{\Delta Ot}$ mice is due to direct regulation of *IL-7*

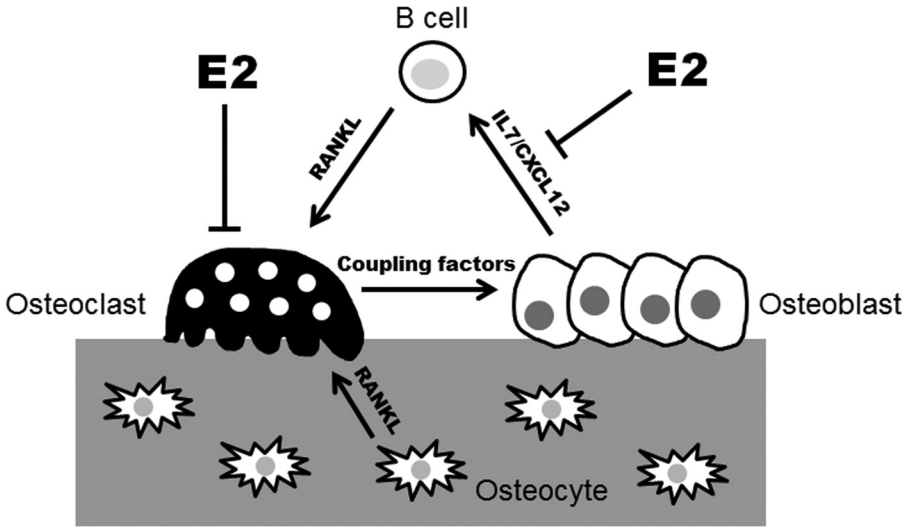

FIGURE 7. **Bone and immune cell interactions during estrogen deficiency.** Estrogens suppress bone resorption by acting directly on osteoclasts. However, the increase in osteoclast number during estrogen deficiency requires RANKL from both osteocytes and B cells. The increase in B cells that occurs with estrogen deficiency may contribute to osteoclast formation and may be a consequence of the increase in osteoblast number. It is also possible that the expression of cytokines that support B cell formation by osteoblast-lineage cells is suppressed by estrogen.

and *CXCL-12* genes by RANK signaling. However, we did not observe any change in the levels of either *IL-7* or *CXCL-12* mRNA in bone marrow osteoblasts treated with 100 ng/ml RANKL for 24 h (data not shown), arguing against this scenario.

An increase in B cell number is one of the most consistently observed changes in the bone marrow of estrogen-deficient mice (10, 11, 39). Because this increase is coincident with bone loss and because of the juxtaposition of the bone marrow with bone matrix, Suda and co-workers (40) proposed a causal link between the increase in B cell number and the elevated bone resorption caused by estrogen deficiency. Consistent with their idea, administration of IL-7 to estrogen-replete mice was sufficient to increase not only B cell number but also osteoclast number and bone resorption (40). Mature B cells, however, do not appear to be required as similar amounts of bone were lost after ovariectomy in mice with and without mature B cells (41).

B cells may also contribute to the bone loss that occurs in estrogen-deficient humans. Comparison of bone marrow cells from pre-menopausal, post-menopausal, and estrogen-treated post-menopausal women revealed higher levels of RANKL on the surface of B cells in post-menopausal women not receiving estradiol (42). Although an increase in total B cells was not noted in this study, a second study reported a decrease in the number of bone marrow cells expressing RANKL in post-menopausal women after 3 weeks of estradiol treatment (43). Although the identity of the RANKL-expressing cells in this latter study was not determined, the cells were in the flow-cytometric fraction that contains lymphocytes. Consistent with the idea that B cells may increase in estrogen-deficient women, administration of estradiol or raloxifene to post-menopausal women reduces circulating levels of IL-7 (44, 45).

If the increase in B cell number contributes to the increase in osteoclast number, our current study demonstrates that they do this by some mechanism other than by acting as osteoclast progenitors. Although multiple studies utilizing purified B cells have demonstrated that these preparations can produce osteoclasts *in vitro*, our lineage-tracing studies demonstrate that B cells cannot act as osteoclast progenitors *in vivo*. Based on this and on our *in vitro* lineage-tracing studies we conclude that the osteoclasts formed after culture of isolated B cells must be derived from contaminating myeloid cells. A similar conclusion was reached by Aguila and co-workers (46), who demonstrated that more highly purified B cell preparations failed to generate osteoclasts *in vitro*.

The current results together with earlier findings regarding RANKL produced by B cells and ERα produced by osteoclasts suggest the following model to explain the cancellous bone loss caused by estrogen deficiency (Fig. 7). First, loss of estrogen action directly on osteoclasts allows their number to increase, which in turn elevates osteoblast number. RANKL produced by osteocytes is permissive for this increase. The increase in remodeling increases the number of B lymphocytes in the bone marrow due to elevated production of factors such as IL-7 and CXCL-12 by osteoblast-lineage cells. The increase in these factors may be due to an increased number of osteoblasts as well as to loss of estrogen inhibition of their expression in stromal cells. The increase in B cell number then introduces additional RANKL into the system, which promotes even more osteoclast formation, resulting in a feed-forward loop and bone loss. The ability of B cell RANKL to promote bone resorption is highlighted by the recent finding that activation of mTOR in B cells is sufficient to increase RANKL production in these cells and stimulate osteoclast formation and bone loss (47). Overall, our results support the contention that bone loss due to estrogen deficiency in mice results from dysregulation of a complex set of interactions between the skeletal and hematopoietic systems.

Experimental Procedures

Animals—To disrupt *Tnfsf11* in mature osteoblasts and osteocytes, Tnfsf11$^{f/f}$ mice (6) were crossed with mice harboring a *Dmp1-Cre* transgene (48). Mice used in the ovariectomy experiments were littermates generated by crossing Tnfsf11$^{f/f}$ with Dmp1-Cre;Tnfsf11$^{f/f}$ mice. To disrupt *Esr1* in B lymphocytes, Esr1$^{f/f}$ mice (49) were crossed with CD19-Cre mice (25).

Mice used in the ovariectomy experiments were littermates generated by crossing $Esr1^{f/f}$ mice with CD19-Cre;$Esr1^{f/f}$ mice. Lineage-tracing studies were performed in tdTomato Cre-reporter mice (line Ai9) (50) after crossing with either CD19-Cre or LysM-Cre (51) mice. All lines used in this study were backcrossed into the C57BL/6J genetic background for >10 generations before the crosses described here. Offspring were genotyped by PCR using the following primer sequences: Cre-for, 5′-GCGGTCTGGCAGTAAAAACTATC-3′; Cre-rev, 5′-GTGAAACAGCATTGCTGTCACTT-3′ (product size 102 bp); RANKLflox-for, 5′-CTGGGAGCGCAGGTTAAATA-3′; RANKLflox-rev, 5′-GCCAATAATTAAAATACTGCAGGAAA-3′ (product size 108 bp (wild type) and 251 bp (floxed allele)); $ER\alpha^{f/f}$-for, 5′-TCGTTTTGAATTAATTATGAATGTCTG-3′, $ER\alpha^{f/f}$-rev, 5′-TTCATGTGTTGTGCAAATAGC-3′ (product size 647 bp (wild type) and 933 bp (floxed allele)); oIMR9020, 5′-AAGGGAGCTGCAGTGGAGTA-3′; oIMR9021, 5′-CCGAAAATCTGTGGGAAGTC-3′; oIMR9103, 5′-GGCATTAAAGCAGCGTATCC-3′; oIMR9105, 5′-CTGTTCCTGTACGGCATGG-3′ (product size 297 bp (wild type) and 196 bp (tdTomato)). Sham and ovariectomy operations were performed at 6–7 months of age for gene deletion studies and at 3 months of age for lineage-tracing studies. Mice were assigned to ovariectomy or sham groups based on bone mineral density of the lumbar spine. Specifically, mice were rank-ordered by bone mineral density and then assigned the number 1 or 2, successively. Animals with the same number were assigned to the same operation group to give identical group means. Mice were euthanized 6 weeks after the operations. All studies involving mice were approved by the Institutional Animal Care and Use Committees of the University of Arkansas for Medical Sciences and the Central Arkansas Veterans Healthcare System.

Microcomputed Tomography (μCT)—Cortical and trabecular architecture was measured by μCT of the fourth lumbar vertebra and femur. Soft tissue was removed from L4 vertebra or femurs, which were then fixed in Millonig's 10% formalin for 24 h and transferred gradually from 70% to 100% ethanol. Bones were loaded into a 12.3-mm-diameter scanning tube and imaged using a μCT (model μCT40, Scanco Biomedical, Bruttisellen, Switzerland). Scans were integrated into three-dimensional voxel images (1024 × 1024 pixels) and a Gaussian filter (sigma = 0.8, support = 1) was used to reduce signal noise. A threshold of 200 was applied to all scans at medium resolution (E = 55 peak kilovoltage, I = 145 μA, integration time = 200 ms). The entire vertebral body was scanned with a transverse orientation. The cortical bone and the primary spongiosa were manually excluded from the analyses. All trabecular measurements were made by drawing contours every 10–20 slices and using voxel counting for bone volume per tissue volume and sphere-filling distance transformation indices without presumptions about the bone shape as a rod or plate for trabecular microarchitecture. Cortical thickness was measured at the femoral mid-diaphysis. Calibration and quality control were performed weekly using five density standards, and spatial resolution was verified monthly using a tungsten wire rod. Beam hardening correction was based on the calibration records.

Flow Cytometry—Bone marrow cells were collected by removing both ends of the femur and flushing out the cells with PBS containing 3% FBS. Bone marrow cells were washed and blocked with anti-mouse CD16/CD32 (mouse BD Fc-block; BD Biosciences) for 5 min. The cells were then stained for 30 min using the following antibodies: anti-CD19-APC-Cy7 (2 μg/ml) and anti-CD45R/B220-PE-Cy7 (2.5 μg/ml) to identify B cells, anti-CD3-FITC (5 μg/ml) to identify T cells, anti-CD11b-APC (0.5 μg/ml) to identify monocytes-macrophages, and anti-TER-119-PerCP/Cy5.5 (0.5 μg/ml) to identify erythroid cells. Stages of B cell development were identified using the following antibodies: anti-B220-FITC (2.5 μg/ml), anti-CD43-PE (2 μg/ml), anti-CD19-APC Cy7 (2 μg/ml), and anti-IgM-BV650 (2 μg/ml). All antibodies were purchased from BD Biosciences. After washing to remove unbound antibodies, samples were analyzed by a BD FACS Aria flow cytometer (BD Biosciences). The data were analyzed using FlowJo Software (FlowJo, LLC, Ashland, OR). Appropriate gates for the cell populations were drawn with guidance of Fluorescence Minus One (FMO) controls (BD Biosciences).

RNA Purification and Gene Expression—Tibal cortical bone was prepared by removing the distal and proximal ends and removing bone marrow cells by centrifugation at 13,000 × *g* for 2 min. Cortical bone was then stored at −80 °C before RNA extraction. Total RNA was purified from bone or isolated cells using TRIzol Reagent (ThermoFisher Scientific) according to the manufacturer's instructions. RNA was quantified using a Nanodrop instrument (ThermoFisher Scientific), and RNA integrity was verified by resolution on 0.8% agarose gels. 500 ng of RNA was then used to synthesize cDNA using the High-Capacity cDNA Reverse Transcription kit (ThermoFisher Scientific) according to the manufacturer's directions. Transcript abundance in the cDNA was measured by quantitative PCR using TaqMan Universal PCR Master Mix (ThermoFisher Scientific) (52). The following Taqman assays were used: *Tnfsf11* (Mm0041908_m1); *Tnfrsf11b* (Mm00435452_m1); *IL-7* (Mm01295803_m1); *CXCL12* (Mm00445553_m1); the house-keeping gene *Mrps2* (forward, 5′-CCCAGGATGGCGACGAT-3′; reverse, 5′-CCGAATGCTGTAATGGCGTAT-3′; probe 5′-FAM-TCCAGAGCAGGATCC-NFQ-3′). Gene expression was calculated using the ΔCt method relative to *Mrps2* levels (53).

Genomic DNA Isolation—The distal and proximal ends of the left femur were removed, and bone marrow cells were flushed out completely with PBS. The surfaces of the bone shafts were scraped with a scalpel to remove the periosteum and then cut into a few small pieces. Bone pieces were decalcified in 14% EDTA for 1 week. Soft tissues were dissected from animals, frozen immediately in liquid nitrogen, and stored at −80 °C. Decalcified bone and soft tissues were digested with proteinase K (0.5 mg/ml in 10 mM Tris, pH 8.0, 100 mM NaCl, 20 mM EDTA, and 1% SDS) at 55 °C overnight. Genomic DNA was then isolated by phenol/chloroform extraction and ethanol precipitation. Two custom Taqman assays were designed for quantifying *Tnfsf11* gene deletion efficiency: one specific for sequences between the loxP sites (forward, 5′-GCCAGTGGACTTACTCAAACCTT-3′; reverse, 5′-GGTAGGGTTCAACTGAAGGGTTTA-3′; probe, 5′-FAM-CCTCCTCCTCATG-

GTTTAGTNFQ-3′) and the other specific for sequences downstream from the 3′ loxP site (forward, 5′-GGTGCCGTG-CATTATCCTAGAC-3′; reverse, 5′-AAGTAATGTGACCC-TTGGAGAACTG-3′; probe, 5′-FAM-CTAGCACACGTG-CCTGCTNFQ-3′).

Histology—Sections for histomorphometry were obtained from lumbar vertebrae (L1-L3) by fixing them for 24 h in Millonig's 10% formalin followed by decalcification in 14% EDTA, pH 7.1, for 1 week, dehydration, paraffin-embedding, and cutting 5-μm longitudinal sections. After removal of paraffin and rehydration, the sections were stained for tartrate-resistant acid phosphatase (TRAP) activity and counterstained with methyl green. The number and the surface of TRAP-positive cells on the cancellous perimeter (osteoclast number and surface) were measured using an Olympus BX53 microscope and Olympus DP73 camera (Olympus Corp.) interfaced with a digitizer tablet with Osteomeasure^{TM} software version 4.1.0.2 (OsteoMetrics Inc). Histomorphometry measurements were made in a blinded fashion. The terminology used in this study has been recommended by the Histomorphometry Nomenclature Committee of the American Society for Bone and Mineral Research (54). Sections for lineage-tracing studies were obtained from lumbar vertebrae by fixing overnight in 4% paraformaldehyde at 4 °C followed by decalcification in 14% EDTA for 1 week and immersion in 30% sucrose for a minimum of 1 day. Bones were then embedded in Cryo-Gel (Electron Microscopy Sciences, Hatfield, PA) for frozen sectioning. 4-μm sections were obtained using a Leica cryostat with tape transfer system (Leica Microsystems LM3050S, Buffalo Grove, IL). The sections were imaged on the Olympus BX53 microscope using a DAPI/FITC/Texas Red triple filter cube. The same sections were subsequently stained for TRAP activity and counterstained with methyl green, after which brightfield images were obtained.

Isolation of B Cells Using Magnetic Beads—B cells were isolated with a magnetic cell isolation system (MACS; Miltenyi Biotec, Bergisch Gladbach, Germany). After the column was flushed with ice-cold PBS, 1% BSA, cells labeled with anti-CD19 antibody-conjugated magnetic beads were applied to the column. Unbound cells were washed out with 3 column volumes of PBS, 1% BSA. The column was further washed with 3 volumes of PBS, 1% BSA. After the steel wool column was removed from the external magnetic field, bound cells were eluted and analyzed by flow cytometry.

Osteoclast Culture—BMMs were prepared as described previously (18). Briefly, bone marrow cells were isolated from tibia and femur by flushing with PBS. Bone marrow cells were plated in α-10 medium (α-minimum Eagle's medium, 10% heat-inactivated FBS, 1% penicillin-streptomycin-L-glutamine solution), and 1/10 volume of CMG 14–12 (conditioned medium supernatant containing recombinant M-CSF at 1 mg/ml) (38) in Petri dishes. Cells were cultured for 4–5 days with fresh media, and CMG 14–12 supernatant was replaced every other day. To generate osteoclasts, BMMs were harvested and re-plated in medium containing 1/100 volume of CMG 14–12 supernatant and 100 ng/ml concentrations of recombinant RANKL and cultured until large multinucleated cells formed (4–6 days). For osteoclastogenesis using CD19+ cell preparations, CD19+ and CD19− cells were isolated using magnetic beads then cultured in the presence of 1/100 volume CMG 14–12 supernatant and 100 ng/ml RANKL. Osteoclast formation was detected after 5 or 8 days.

Statistics—Data were analyzed using SigmaStat (SPSS Science, Chicago, IL). Two-way analysis of variance was used to detect statistically significant treatment effects after determining that the data were normally distributed and exhibited equivalent variances. In some cases log or ranks transformations were used to obtain normally distributed data and equal variance. This was followed by all pairwise comparisons using Tukey's procedure. For experiments involving comparison of only two groups, Student's t test or two-sample test with multiple comparisons was used. p values less than 0.05 were considered as significant. All quantitative results are presented as box and whisker plots in which the boundary of the box closest to zero indicates the 25th percentile, the line within the box marks the median, and the boundary of the box farthest from zero indicates the 75th percentile. Whiskers (error bars) above and below the box indicate the 90th and 10th percentiles, and values outside the 90th and 10th percentiles are shown as individual points.

Author Contributions—Y. F. and C. A. O. designed the experiments. Y. F., M. P., Y. L., and J. X. performed the experiments. Y. F., J. D. T., and C. A. O. analyzed the results. Y. F. and C. A. O. wrote the first draft of the manuscript. All authors edited the manuscript.

Acknowledgments—We thank P. Baltz, A. Warren, I. Gubrij, S. Berryhill, and H. Zhao for technical assistance and M. Almeida, S. Manolagas, and R. Jilka for critical reading of the manuscript.

References

1. Teitelbaum, S. L., and Ross, F. P. (2003) Genetic regulation of osteoclast development and function. *Nat. Rev. Genet.* **4,** 638–649
2. Kong, Y. Y., Yoshida, H., Sarosi, I., Tan, H. L., Timms, E., Capparelli, C., Morony, S., Oliveira-dos-Santos, A. J., Van G, Itie, A., Khoo, W., Wakeham, A., Dunstan, C. R., Lacey, D. L., Mak, T. W., Boyle, W. J., and Penninger, J. M. (1999) OPGL is a key regulator of osteoclastogenesis, lymphocyte development and lymph-node organogenesis. *Nature* **397,** 315–323
3. Fata, J. E., Kong, Y. Y., Li, J., Sasaki, T., Irie-Sasaki, J., Moorehead, R. A., Elliott, R., Scully, S., Voura, E. B., Lacey, D. L., Boyle, W. J., Khokha, R., and Penninger, J. M. (2000) The osteoclast differentiation factor osteoprotegerin-ligand is essential for mammary gland development. *Cell* **103,** 41–50
4. O'Brien, C. A. (2010) Control of RANKL gene expression. *Bone* **46,** 911–919
5. Dallas, S. L., Prideaux, M., and Bonewald, L. F. (2013) The osteocyte: an endocrine cell . . . and more. *Endocr. Rev.* **34,** 658–690
6. Xiong, J., Onal, M., Jilka, R. L., Weinstein, R. S., Manolagas, S. C., and O'Brien, C. A. (2011) Matrix-embedded cells control osteoclast formation. *Nat. Med.* **17,** 1235–1241
7. Nakashima, T., Hayashi, M., Fukunaga, T., Kurata, K., Oh-Hora, M., Feng, J. Q., Bonewald, L. F., Kodama, T., Wutz, A., Wagner, E. F., Penninger, J. M., and Takayanagi, H. (2011) Evidence for osteocyte regulation of bone homeostasis through RANKL expression. *Nat. Med.* **17,** 1231–1234
8. Xiong, J., Piemontese, M., Thostenson, J. D., Weinstein, R. S., Manolagas, S. C., and O'Brien, C. A. (2014) Osteocyte-derived RANKL is a critical mediator of the increased bone resorption caused by dietary calcium deficiency. *Bone* **66,** 146–154

9. Manolagas, S. C., O'Brien, C. A., and Almeida, M. (2013) The role of estrogen and androgen receptors in bone health and disease. *Nat. Rev. Endocrinol.* **9,** 699–712
10. Smithson, G., Beamer, W. G., Shultz, K. L., Christianson, S. W., Shultz, L. D., and Kincade, P. W. (1994) Increased B lymphopoiesis in genetically sex steroid-deficient hypogonadal (hpg) mice. *J. Exp. Med.* **180,** 717–720
11. Masuzawa, T., Miyaura, C., Onoe, Y., Kusano, K., Ohta, H., Nozawa, S., and Suda, T. (1994) Estrogen deficiency stimulates B lymphopoiesis in mouse bone marrow. *J. Clin. Invest.* **94,** 1090–1097
12. Onal, M., Xiong, J., Chen, X., Thostenson, J. D., Almeida, M., Manolagas, S. C., and O'Brien, C. A. (2012) Receptor activator of nuclear factor κB Ligand (RANKL) protein expression by B lymphocytes contributes to ovariectomy-induced bone loss. *J. Biol. Chem.* **287,** 29851–29860
13. Sato, T., Shibata, T., Ikeda, K., and Watanabe, K. (2001) Generation of bone-resorbing osteoclasts from B220(+) cells: its role in accelerated osteoclastogenesis due to estrogen deficiency. *J. Bone Miner. Res.* **16,** 2215–2221
14. Katavić, V., Grcević, D., Lee, S. K., Kalinowski, J., Jastrzebski, S., Dougall, W., Anderson, D., Puddington, L., Aguila, H. L., and Lorenzo, J. A. (2003) The surface antigen CD45R identifies a population of estrogen-regulated murine marrow cells that contain osteoclast precursors. *Bone* **32,** 581–590
15. Blin-Wakkach, C., Wakkach, A., Rochet, N., and Carle, G. F. (2004) Characterization of a novel bipotent hematopoietic progenitor population in normal and osteopetrotic mice. *J. Bone Miner. Res.* **19,** 1137–1143
16. Pugliese, L. S., Gonçalves, T. O., Popi, A. F., Mariano, M., Pesquero, J. B., and Lopes, J. D. (2012) B-1 lymphocytes differentiate into functional osteoclast-like cells. *Immunobiology* **217,** 336–344
17. Manabe, N., Kawaguchi, H., Chikuda, H., Miyaura, C., Inada, M., Nagai, R., Nabeshima, Y., Nakamura, K., Sinclair, A. M., Scheuermann, R. H., and Kuro-o, M. (2001) Connection between B lymphocyte and osteoclast differentiation pathways. *J. Immunol.* **167,** 2625–2631
18. Zhou, J., Ye, S., Fujiwara, T., Manolagas, S. C., and Zhao, H. (2013) Steap4 plays a critical role in osteoclastogenesis in vitro by regulating cellular iron/reactive oxygen species (ROS) levels and cAMP response element-binding protein (CREB) activation. *J. Biol. Chem.* **288,** 30064–30074
19. Perlot, T., and Penninger, J. M. (2012) Development and function of murine B cells lacking RANK. *J. Immunol.* **188,** 1201–1205
20. Parfitt, A. M. (1982) The coupling of bone formation to bone resorption: a critical analysis of the concept and of its relevance to the pathogenesis of osteoporosis. *Metab. Bone Dis. Relat. Res.* **4,** 1–6
21. Terashima, A., Okamoto, K., Nakashima, T., Akira, S., Ikuta, K., and Takayanagi, H. (2016) Sepsis-induced osteoblast ablation causes immunodeficiency. *Immunity* **44,** 1434–1443
22. Wu, J. Y., Purton, L. E., Rodda, S. J., Chen, M., Weinstein, L. S., McMahon, A. P., Scadden, D. T., and Kronenberg, H. M. (2008) Osteoblastic regulation of B lymphopoiesis is mediated by $G\alpha_s$-dependent signaling pathways. *Proc. Natl. Acad. Sci. U.S.A.* **105,** 16976–16981
23. Mansour, A., Anginot, A., Mancini, S. J., Schiff, C., Carle, G. F., Wakkach, A., and Blin-Wakkach, C. (2011) Osteoclast activity modulates B-cell development in the bone marrow. *Cell Res.* **21,** 1102–1115
24. Greenbaum, A., Hsu, Y. M., Day, R. B., Schuettpelz, L. G., Christopher, M. J., Borgerding, J. N., Nagasawa, T., and Link, D. C. (2013) CXCL12 in early mesenchymal progenitors is required for haematopoietic stem-cell maintenance. *Nature* **495,** 227–230
25. Rickert, R. C., Roes, J., and Rajewsky, K. (1997) B lymphocyte-specific, Cre-mediated mutagenesis in mice. *Nucleic Acids Res.* **25,** 1317–1318
26. Kondoh, S., Inoue, K., Igarashi, K., Sugizaki, H., Shirode-Fukuda, Y., Inoue, E., Yu, T., Takeuchi, J. K., Kanno, J., Bonewald, L. F., and Imai, Y. (2014) Estrogen receptor α in osteocytes regulates trabecular bone formation in female mice. *Bone* **60,** 68–77
27. Windahl, S. H., Börjesson, A. E., Farman, H. H., Engdahl, C., Movérare-Skrtic, S., Sjögren, K., Lagerquist, M. K., Kindblom, J. M., Koskela, A., Tuukkanen, J., Divieti Pajevic, P., Feng, J. Q., Dahlman-Wright, K., Antonson, P., Gustafsson, J. Å., Ohlsson, C. (2013) Estrogen receptor-α in osteocytes is important for trabecular bone formation in male mice. *Proc. Natl. Acad. Sci. U.S.A.* **110,** 2294–2299
28. Li, X., Ominsky, M. S., Stolina, M., Warmington, K. S., Geng, Z., Niu, Q. T., Asuncion, F. J., Tan, H. L., Grisanti, M., Dwyer, D., Adamu, S., Ke, H. Z., Simonet, W. S., and Kostenuik, P. J. (2009) Increased RANK ligand in bone marrow of orchiectomized rats and prevention of their bone loss by the RANK ligand inhibitor osteoprotegerin. *Bone* **45,** 669–676
29. Proell, V., Xu, H., Schüler, C., Weber, K., Hofbauer, L. C., and Erben, R. G. (2009) Orchiectomy upregulates free soluble RANKL in bone marrow of aged rats. *Bone* **45,** 677–681
30. Xiong, J., Piemontese, M., Onal, M., Campbell, J., Goellner, J. J., Dusevich, V., Bonewald, L., Manolagas, S. C., and O'Brien, C. A. (2015) Osteocytes, not osteoblasts or lining cells, are the main source OF the RANKL required for osteoclast formation in remodeling bone. *PLoS ONE* **10,** e0138189
31. Zhang, J., and Link, D. C. (2016) Targeting of mesenchymal stromal cells by cre-recombinase transgenes commonly used to target osteoblast lineage cells. *J Bone Miner. Res.* 10.1002/jbmr.2877
32. Zhu, J., Garrett, R., Jung, Y., Zhang, Y., Kim, N., Wang, J., Joe, G. J., Hexner, E., Choi, Y., Taichman, R. S., and Emerson, S. G. (2007) Osteoblasts support B-lymphocyte commitment and differentiation from hematopoietic stem cells. *Blood* **109,** 3706–3712
33. Teufel, S., Grötsch, B., Luther, J., Derer, A., Schinke, T., Amling, M., Schett, G., Mielenz, D., and David, J. P. (2014) Inhibition of bone remodeling in young mice by bisphosphonate displaces the plasma cell niche into the spleen. *J. Immunol.* **193,** 223–233
34. Sato, T., Watanabe, K., Masuhara, M., Hada, N., and Hakeda, Y. (2007) Production of IL-7 is increased in ovariectomized mice, but not RANKL mRNA expression by osteoblasts/stromal cells in bone, and IL-7 enhances generation of osteoclast precursors in vitro. *J. Bone Miner. Metab.* **25,** 19–27
35. Weitzmann, M. N., Roggia, C., Toraldo, G., Weitzmann, L., and Pacifici, R. (2002) Increased production of IL-7 uncouples bone formation from bone resorption during estrogen deficiency. *J. Clin. Invest.* **110,** 1643–1650
36. Smithson, G., Medina, K., Ponting, I., and Kincade, P. W. (1995) Estrogen suppresses stromal cell-dependent lymphopoiesis in culture. *J. Immunol.* **155,** 3409–3417
37. Mizoguchi, T., Pinho, S., Ahmed, J., Kunisaki, Y., Hanoun, M., Mendelson, A., Ono, N., Kronenberg, H. M., and Frenette, P. S. (2014) Osterix marks distinct waves of primitive and definitive stromal progenitors during bone marrow development. *Dev. Cell* **29,** 340–349
38. Takeshita, S., Kaji, K., and Kudo, A. (2000) Identification and characterization of the new osteoclast progenitor with macrophage phenotypes being able to differentiate into mature osteoclasts. *J. Bone Miner. Res.* **15,** 1477–1488
39. Kincade, P. W., Medina, K. L., and Smithson, G. (1994) Sex hormones as negative regulators of lymphopoiesis. *Immunol. Rev.* **137,** 119–134
40. Miyaura, C., Onoe, Y., Inada, M., Maki, K., Ikuta, K., Ito, M., and Suda, T. (1997) Increased B-lymphopoiesis by interleukin 7 induces bone loss in mice with intact ovarian function: similarity to estrogen deficiency. *Proc. Natl. Acad. Sci. U.S.A.* **94,** 9360–9365
41. Li, Y., Li, A., Yang, X., and Weitzmann, M. N. (2007) Ovariectomy-induced bone loss occurs independently of B cells. *J. Cell. Biochem.* **100,** 1370–1375
42. Eghbali-Fatourechi, G., Khosla, S., Sanyal, A., Boyle, W. J., Lacey, D. L., and Riggs, B. L. (2003) Role of RANK ligand in mediating increased bone resorption in early postmenopausal women. *J. Clin. Invest.* **111,** 1221–1230
43. Taxel, P., Kaneko, H., Lee, S. K., Aguila, H. L., Raisz, L. G., and Lorenzo, J. A. (2008) Estradiol rapidly inhibits osteoclastogenesis and RANKL expression in bone marrow cultures in postmenopausal women: a pilot study. *Osteoporos. Int.* **19,** 193–199
44. Yasui, T., Saijo, A., Uemura, H., Matsuzaki, T., Tsuchiya, N., Yuzurihara, M., Kase, Y., and Irahara, M. (2009) Effects of oral and transdermal estrogen therapies on circulating cytokines and chemokines in postmenopausal women with hysterectomy. *Eur. J Endocrinol.* **161,** 267–273
45. Yasui, T., Uemura, H., Hyodo, S., Yamada, M., Yamamoto, S., Maegawa, M., Tsuchiya, N., Noguchi, M., Yuzurihara, M., Kase, Y., and Irahara, M. (2009) Raloxifene reduces circulating levels of interleukin-7 and monocyte chemoattractant protein-1 in postmenopausal women. *Atherosclerosis* **204,** 471–475

46. Jacquin, C., Gran, D. E., Lee, S. K., Lorenzo, J. A., and Aguila, H. L. (2006) Identification of multiple osteoclast precursor populations in murine bone marrow. *J. Bone Miner. Res.* **21,** 67–77
47. Xu, S., Zhang, Y., Liu, B., Li, K., Huang, B., Yan, B., Zhang, Z., Liang, K., Jia, C., Lin, J., Zeng, C., Cai, D., Jin, D., Jiang, Y., and Bai, X. (2016) Activation of mTORC1 in B lymphocytes promotes osteoclast formation via regulation of beta-catenin and RANKL/OPG. *J. Bone Miner. Res.* **31,** 1320–1333
48. Lu, Y., Xie, Y., Zhang, S., Dusevich, V., Bonewald, L. F., and Feng, J. Q. (2007) DMP1-targeted Cre expression in odontoblasts and osteocytes. *J. Dent. Res.* **86,** 320–325
49. Martin-Millan, M., Almeida, M., Ambrogini, E., Han, L., Zhao, H., Weinstein, R. S., Jilka, R. L., O'Brien, C. A., and Manolagas, S. C. (2010) The estrogen receptor-α in osteoclasts mediates the protective effects of estrogens on cancellous but not cortical bone. *Mol. Endocrinol.* **24,** 323–334
50. Madisen, L., Zwingman, T. A., Sunkin, S. M., Oh, S. W., Zariwala, H. A., Gu, H., Ng, L. L., Palmiter, R. D., Hawrylycz, M. J., Jones, A. R., Lein, E. S., and Zeng, H. (2010) A robust and high-throughput Cre reporting and characterization system for the whole mouse brain. *Nat. Neurosci.* **13,** 133–140
51. Clausen, B. E., Burkhardt, C., Reith, W., Renkawitz, R., and Förster, I. (1999) Conditional gene targeting in macrophages and granulocytes using LysMcre mice. *Transgenic Res.* **8,** 265–277
52. O'Brien, C. A., Jilka, R. L., Fu, Q., Stewart, S., Weinstein, R. S., and Manolagas, S. C. (2005) IL-6 is not required for parathyroid hormone stimulation of RANKL expression, osteoclast formation, and bone loss in mice. *Am. J. Physiol. Endocrinol. Metab.* **289,** E784–E793
53. Livak, K. J., and Schmittgen, T. D. (2001) Analysis of relative gene expression data using real-time quantitative PCR and the $2(-\Delta\Delta C(T))$ method. *Methods* **25,** 402–408
54. Dempster, D. W., Compston, J. E., Drezner, M. K., Glorieux, F. H., Kanis, J. A., Malluche, H., Meunier, P. J., Ott, S. M., Recker, R. R., and Parfitt, A. M. (2013) Standardized nomenclature, symbols, and units for bone histomorphometry: a 2012 update of the report of the ASBMR histomorphometry nomenclature committee. *J. Bone Miner. Res.* **28,** 2–17